HHS Public Access

Author manuscript

Dev Cell. Author manuscript; available in PMC 2010 August 01.

Published in final edited form as:

Dev Cell. 2009 August ; 17(2): 175–186. doi:10.1016/j.devcel.2009.06.017.

Integrin-α9 is required for fibronectin matrix assembly during lymphatic valve morphogenesis

Eleni Bazigou[1], **Sherry Xie**[1], **Chun Chen**[2], **Anne Weston**[3], **Naoyuki Miura**[4], **Lydia Sorokin**[5], **Ralf Adams**[6,7], **Andrés F. Muro**[8], **Dean Sheppard**[2], and **Taija Makinen**[1,*]

[1] Lymphatic Development Laboratory, Cancer Research UK London Research Institute, 44 Lincoln's Inn Fields, London WC2A 3PX, United Kingdom

[2] Lung Biology Center, UCSF, San Francisco CA 94143-2922, USA

[3] Electron Microscopy Unit, Cancer Research UK London Research Institute, 44 Lincoln's Inn Fields, London WC2A 3PX, United Kingdom

[4] Department of Biochemistry, Hamamatsu University School of Medicine, Hamamatsu 431-3192, Japan

[5] Institute for Physiological Chemistry and Pathobiochemistry, Münster University, 48149 Münster, Germany

[6] Vascular Development Laboratory, Cancer Research UK London Research Institute, 44 Lincoln's Inn Fields, London WC2A 3PX, United Kingdom

[7] Max–Planck–Institute for Molecular Biomedicine, Department of Tissue Morphogenesis, and University of Münster, Faculty of Medicine, 48149 Münster, Germany

[8] International Centre for Genetic Engineering and Biotechnology, 34012 Trieste, Italy

Summary

Dysfunction of lymphatic valves underlies human lymphedema, yet the process of valve morphogenesis is poorly understood. Here, we show that during embryogenesis lymphatic valve leaflet formation is initiated by upregulation of integrin-α9 expression and deposition of its ligand, fibronectin-EIIIA (FN-EIIIA), in the extracellular matrix. Endothelial cell specific deletion of *Itga9* (encoding integrin-α9) in mouse embryos results in the development of rudimentary valve leaflets, characterized by disorganized FN matrix, short cusps and retrograde lymphatic flow. Similar morphological and functional defects are observed in mice lacking the EIIIA domain of FN. Mechanistically, we demonstrate that in primary human lymphatic endothelial cells the integrin-α9-EIIIA interaction directly regulates FN fibril assembly, which is essential for the

* Corresponding author: taija.makinen@cancer.org.uk, Phone: +44 207 269 3459, Fax: +44 207 269 3417.

Author contributions: E.B. and T.M. designed research; E.B., S.X., C.C. and A.W. performed research; N.M., L.S., R.A., A.M. and D.S. contributed reagents; E.B., S.X., C.C., A.W. and T.M. analysed data; and E.B. and T.M. wrote the paper.

formation of the extracellular matrix core of valve leaflets. Our findings reveal an important role for integrin-α9 signaling during lymphatic valve morphogenesis and implicate it as a candidate gene for primary lymphedema caused by valve defects.

Introduction

The lymphatic vasculature forms a network of blind-ended capillaries that collect protein rich fluid from the interstitial space and drain it via collecting vessels first into lymph nodes and then to larger lymphatic ducts, which connect to the venous system (Alitalo et al., 2005; Jurisic and Detmar, 2009). The major functions of the lymphatic vasculature are to maintain tissue fluid balance, provide immune surveillance through transport of leukocytes and antigen-presenting dendritic cells and participate in fat absorption (Alitalo et al., 2005; Jurisic and Detmar, 2009).

Congenital malformation of the lymphatic system such as vessel hypoplasia and valve defects cause primary lymphedema, which is usually a progressive and lifelong condition, characterized by gross swelling of the affected limb accompanied by fibrosis and susceptibility to infections (Alitalo et al., 2005; Jurisic and Detmar, 2009). The management of symptoms is based on physiotherapy and compression garments as at present no effective treatment for lymphedema exists. Several genes, including *Vegfr3*, *Foxc2 and Sox18*, which were shown to regulate developmental lymphangiogenesis in mice (Francois et al., 2008; Karkkainen et al., 2001; Petrova et al., 2004), have been implicated in human lymphedema. Kinase inactivating mutations in the *VEGFR-3* gene lead to Milroy's disease (Ferrell et al., 1998), while mutations in the transcription factors *FOXC2* and *SOX18* are the underlying genetic causes of lymphedema-distichiasis and hypotrichosis-lymphedema-telangiectasia, respectively (Finegold et al., 2001; Irrthum et al., 2003). Interestingly, defective luminal valves observed as a consequence of loss of *FOXC2* function (Petrova et al., 2004) highlights the critical role of valves in maintaining unidirectional lymphatic flow. While the mechanisms of lymphatic valve morphogenesis remain poorly characterized, it has been well established that the interactions between the blood endothelial cells and their surrounding extracellular matrix (ECM), organized to facilitate valve function, are of key importance in regulating heart valve development and cardiac function, and consequently, heart valve disease (Armstrong and Bischoff, 2004; Lincoln et al., 2006). Similarly, ultrastructural analyses of lymphatic valves have demonstrated a close association between ECM and lymphatic endothelial cells in the valve leaflets (Lauweryns and Boussauw, 1973; Navas et al., 1991). These findings suggest that the ECM has important functions in controlling endothelial cell signalling and could also provide structural integrity during lymphatic valve morphogenesis.

Cell-matrix adhesion receptors, such as integrins, play essential roles in developmental processes that involve close interactions between the cells and their surrounding ECM. Integrins are heterodimeric transmembrane receptors composed of α and β subunits. Their extracellular domains bind to the ECM molecules while the cytoplasmic domains associate with the actin cytoskeleton and affiliated proteins, thereby providing a link between the external and internal environment of the cell (Geiger et al., 2001). In addition to mediating

attachment to their respective ECM ligand(s), integrins have specialized signaling functions and they can regulate gene expression as well as cell shape, migration, proliferation and survival. Furthermore, integrin binding to ECM is not only required for transducing signals from the matrix to cells but this interaction also initiates responses that allow the cells to organize and remodel the matrix (Leiss et al., 2008). Despite an apparent redundancy in their ligand-binding specificities, with several ECM molecules being ligands for more than one integrin, genetic studies have demonstrated distinct functions for individual integrins. Fibronectin (FN) receptors integrin-α5β1 and -α4β1, as well as components of the ECM, such as FN, play critical roles in the development of the blood vasculature (Hynes, 2007). However, knowledge of the expression and function of integrins and the ECM in the lymphatic vasculature is limited (Avraamides et al., 2008).

Here we show that a member of the integrin-family, integrin-α9 (encoded by *Itga9*), was predominantly expressed in the endothelial cells of the lymphatic valve. Interestingly, *Itga9* deficiency in mice led to specific defects in the formation of luminal valves, which resulted in retrograde lymphatic flow and impaired fluid transport. We provide *in vivo* and *in vitro* evidence for the requirement of integrin-α9 interaction with its specific ligand, fibronectin-EIIIA (FN-EIIIA, also called EDA), in regulating FN matrix assembly and thereby identify an unexpected *in vivo* function for an integrin-EIIIA interaction. Collectively, our findings demonstrate an important role for integrin signaling in lymphatic valve development and provide novel insight into the previously undescribed morphogenetic process of lymphatic valve morphogenesis. As lymphatic valve defects manifested in adults are likely to have origins in valve development, integrin-α9 is a candidate gene for primary human lymphedema caused by lymphatic valve defects.

Results

Integrin-α9 is expressed in mature and developing lymphatic valves

We surveyed expression of several integrins by immunofluorescence to determine which of these molecules might function during lymphatic valve formation. Whole-mount staining of adult skin using antibodies against specific α-subunits revealed low levels of integrin-α5 and -α6 expression in lymphatic endothelia and in the valve, while no apparent staining was detected using antibodies against integrin-α1, -α2 or -α4 (data not shown). In contrast, staining with integrin-α9 antibodies strongly highlighted the cells constituting the luminal valve (Figures 1A and 1B). In agreement with previous studies (Huang et al., 2000), no integrin-α9 expression was detected in the blood vessel endothelia (data not shown).

Since integrin-α9 appeared to be the predominant α-subunit expressed in lymphatic endothelia and valves, we further characterized its expression pattern in developing vessels and aimed our study at determining its function in valve morphogenesis. During mouse development, the formation of valved collecting vessels occurs in late embryonic and early postnatal life through remodelling of a primitive lymphatic capillary network (Figures 1C-1E; (Makinen et al., 2005; Norrmen et al., 2009)). At embryonic day (E)16, mesenteric lymphatic vessels form a vascular plexus that is LYVE-1 positive and does not contain valves (Figures 1C and 1F). However, defined clusters of cells expressing high levels of Prox1 (Figure 1F) and FoxC2 (data not shown) transcription factors are indicative of

initiation of valve formation (Norrmen et al., 2009). At this stage integrin-α9 expression was low in lymphatic endothelia (Figures 1F and 1G), while higher expression was detected in scattered cells in the surrounding tissue (data not shown) and in vascular SMCs around the blood vessels (Figures 1F and 1G, arrowheads). At E17, the lymphatic vessels formed constrictions that showed elevated *Vegfr3*-lacZ reporter activity (Figure 1D) and contained endothelial cells expressing high levels of FoxC2 (Figure 1H), Prox1 (data not shown) and integrin-α9 (Figures 1H and 1I). At E18, integrin-α9 was present in the endothelial cells of developed valve leaflets (Figures 1J and 1K). Taken together, these expression data suggest that integrin-α9 upregulation in lymphatic endothelia correlated with the initiation of valve leaflet formation.

Itga9 deficient mice display abnormal lymphatic valves

To investigate the physiological function of integrin-α9 in lymphatic valves we analysed *Itga9* deficient mice. These mice were reported to die perinatally of respiratory failure, caused by the presence of bilateral chylothorax (Huang et al., 2000), however the potential lymphatic vascular defects remained unknown. Analysis of chyle-filled mesenteric collecting vessels revealed characteristic V-shaped valves in wild-type neonates (Figures 2A and 2A′). In contrast, *Itga9* mutant mice displayed fewer and morphologically abnormal valves (Figures 2B and 2B′). Staining with an antibody against PECAM-1, which is strongly expressed in endothelial cells forming the valve leaflets (Figure 2C), demonstrated that most of the mutant valves appeared as horizontal constrictions rather than V-shaped structures (Figures 2D, 2E and 2F). Leakage of chylous fluid from the mesenteric vessels further indicated that they were dysfunctional (arrowhead in Figure 2B). The defects in *Itga9* deficient mice were specific to lymphatic valves since we observed apparently normal development and gross morphology of the lymphatic vasculature in all tissues that were examined (Figures S1A-S2H).

Examination of longitudinal transmission electron microscopy sections of the valves of mesenteric lymphatic vessels revealed leaflets consisting of two endothelial layers with a central connective tissue core (Figures 2G, 2I, 2K; (Lauweryns and Boussauw, 1973; Navas et al., 1991)). The endothelial cells of the wild-type valve leaflets formed long, overlapping cell-cell junctions, and they were tightly attached to the matrix core (Figures 2G and 2I). In the *Itga9*$^{-/-}$ vessels the cusps of the valves were shorter with fewer endothelial cells (Figures 2H and 2K). The disorganized or absent matrix core in between the basal sides of the endothelial cells was associated with the separation of the opposite endothelial surfaces (Figure 2J). These results suggest that integrin-α9 function is essential for the formation of the defined ECM core of a valve leaflet.

Retrograde lymph flow and impaired fluid transport in *Itga9*$^{-/-}$ mice

Luminal valves have an important role in establishing unidirectional lymphatic flow. To evaluate if lymphatic function is compromised in the *Itga9*$^{-/-}$ mice, we investigated uptake and transport of subcutaneously injected large-molecular-weight fluorescent dextran. In wild-type mice the FITC-dextran injected into the forelimb footpad was rapidly drained into the valved dermal collecting lymphatic vessels, which were visualized proximal to the injection site (Figure 3A). In contrast, in the *Itga9* mutant skin the dye labeled a vessel

network (Figure 3B), suggesting retrograde lymphatic flow from the collecting vessels to the pre-collector vessel branches (Makinen et al., 2005; Petrova et al., 2004). In addition, the dye showed leakage into the surrounding tissue and the transport from the injection site to the lymph nodes and the thoracic duct was impaired (Figures S2A-S2D). We also analyzed the lymphatic drainage after subcutaneous injection of FITC-conjugated *Lycopersicum Esculentum* lectin (LEL), which binds to the surface of lymphatic endothelial cells, in particular in the valves (Tammela et al., 2007) (Figure 3C). In the *Itga9* mutants valve regions were identified by stronger lectin staining, however, the valves were abnormal and often lacked obvious leaflets (Figures 3D and 3E). Together, the above data show that *Itga9* deficient mice display specific defects in valve morphogenesis, which result in retrograde lymphatic flow and impaired fluid transport.

Integrin-α9 is required tissue-autonomously in endothelia for lymphatic valve development

To examine if integrin-α9 has a tissue-autonomous function in lymphatic endothelia during valve development we deleted its expression specifically in endothelial cells by crossing the floxed $Itga9^{lx}$ mice (Singh et al., 2008) with *Tie2-Cre* animals (Koni et al., 2001). The homozygous *Tie2-Cre;*$Itga9^{lx/lx}$ mice displayed chylothorax (data not shown) and reduced number of lymphatic valves (Figures S3A and S3B). The few valves that were detected displayed abnormal leaflets, as visualized by staining for an ECM molecule Laminin-α5 (Figures 4A-4D).

We next asked whether integrin-α9 is also essential for the maintenance of the valves. We used *VE-cadherin-CreER*^{T2} mice, which allow tamoxifen-regulated activation of Cre in both blood and lymphatic endothelia (R. Adams, unpublished; Figures S3C and S3D). To induce *Itga9* gene deletion in mature valves, 4-hydroxytamoxifen (4-OHT) was injected into control $Itga9^{lx/+}$ (Figures 4E-4H) and *VE-cadherin-CreER*^{T2};$Itga9^{lx/lx}$ (Figures 4I-4L) mice at P1, when most of the valves are fully developed, and the vessels were analysed at P7. In 4-OHT treated *VE-cadherin-CreER*^{T2};$Itga9^{lx/lx}$ vessels integrin-α9 expression was lost from lymphatic endothelia (Figure 4K). However, the valve leaflets appeared normal (Figures 4I and 4J), and integrin-α9 negative endothelial cells remained attached to the matrix core (Figures 4I, 4K and 4L), suggesting that integrin-α9 is dispensable for stable adhesion of endothelial cells in fully developed valves. Together, these results suggest that integrin-α9 is required tissue-autonomously in endothelia for the development of lymphatic valve leaflets, while it is not essential for maintaining valve structure and endothelial cell adhesion in mature valves.

Integrin-α9 ligand, fibronectin-EIIIA, is expressed in the developing lymphatic valves

To examine the function of integrin-α9 in the formation of valve leaflets we investigated the expression and localization of its ligands, including Tenascin-C (TNC), Osteopontin (OPN) and fibronectin containing the EIIIA domain (FN-EIIIA) (Liao et al., 2002; Yokosaki et al., 1998; Yokosaki et al., 1999) in the developing lymphatic vessels. Confocal longitudinal cross section of a valve from E18.5 mesenteric vessels revealed expression of integrin-α9 and its ligand TNC on both luminal and abluminal sides of the valve endothelial cells (Figures S4A-S4C), while no staining was seen for OPN (data not shown). Interestingly,

unlike FN, which was detected in all lymphatic vessel basement membrane (Figures S4D-S4F), FN-EIIIA showed localization restricted to the valve matrix core (Figures S4G-S4I).

To gain further insight into the role of FN-EIIIA we analysed its expression during different stages of lymphatic valve development so as to determine the relationship between integrin-α9 expression and ECM deposition. At E16, prior to upregulation of integrin-α9 expression (Figure 5A), Laminin-α5 was found deposited at specific sites along the vessel (Figures 5A), whereas no fibrous staining for FN-EIIIA was detected (data not shown). Induction of integrin-α9 expression correlated with appearance of continuous FN-EIIIA fibers at sites of developing valves (Figures 5B), which were identified by Laminin-α5 positive matrix (Figure 5C) and the presence of cells expressing high levels of Prox1 (Figure 5D). During initial steps of valve development FN-EIIIA and Laminin-α5 showed a similar localization (Figure 5C). However, during leaflet elongation Laminin-α5 was found in the entire valve matrix core while FN-EIIIA fibers were concentrated on the free edges of the leaflets (Figures 5E and 5E′). Similar to what has been reported for other tissues (Pagani et al., 1991), FN-EIIIA expression was progressively down-regulated in postnatal lymphatic vasculature. While prominent FN-EIIIA fibers were detected in mesenteric lymphatic valves at P3 (data not shown), only weak staining was observed at P9 (Figures S4J-S4L) and no fibers were seen in adult valves (see Figure 6D). These expression data suggest that FN-EIIIA is primarily involved during embryogenesis and that it has a role in the formation and extension of the valve leaflets.

Defective FN-EIIIA matrix assembly and valve leaflet formation in *Itga9*$^{-/-}$ mice

We next examined valve morphogenesis in *Itga9*$^{-/-}$ embryos. X-Gal staining of mesenteric lymphatic vessels in E16 *Itga9*$^{-/-}$;*Vegfr3*$^{lz/+}$ embryos revealed normal vascular networks (Figure S5A). Consistent with the reduced number of valves observed in postnatal *Itga9*$^{-/-}$ vessels, at E17 the number of *Vegfr3*-lacZ positive constrictions (Figures S5B-S5E), that contained clusters of cells expressing high levels of Prox1 and FoxC2 was reduced when compared to the wild-type (Figures S5F and S5G and data not shown). In addition, staining of mutant valves for FN-EIIIA revealed only few short fibers (Figures 5F-5G′). Cross section view through the valve showed a fibrous matrix in wild-type vessels (Figure 5H). In contrast, the underdeveloped leaflets in *Itga9* deficient vessels displayed predominantly a disrupted punctuate and discontinuous pattern (Figures 5I), suggesting that FN-EIIIA failed to assemble into continuous fibers. Taken together, the disorganized FN-EIIIA matrix in *Itga9* deficient vessels and the subsequent arrest in valve development suggest that the defect in valve formation in *Itga9*$^{-/-}$ mice is due to interaction between integrin-α9 and its specific ligand (Figure 5J).

Fibronectin-EIIIA is required for normal development of lymphatic valve leaflets

To test directly if FN-EIIIA, or the other integrin-α9 binding ECM molecules, has a function in valve formation, we analyzed the lymphatic vessels in *Tnc, Opn* and *Fn-EIIIA* deficient mice (Forsberg et al., 1996; Liaw et al., 1998; Muro et al., 2003). Both *Tnc* and *Opn* deficient mice displayed apparently normal lymphatic vasculature and lymphatic valves (Figures S6A-S6F), however, mice deficient for *Fn-EIIIA* partially recapitulated the integrin-α9 mutant phenotype. Quantification of Laminin-α5 positive valve structures in mesenteric

lymphatic vessels of newborn mice showed a 1.5-fold reduction in the number of valves in *Fn-EIIIA*$^{-/-}$ mice when compared to the wild-type ($p = 0.0026$ (Mann-Whitney test), Figure 6A; Table S1). Notably, 76% of the valves in *Fn-EIIIA*$^{-/-}$ mice displayed abnormal matrix ring appearance or underdeveloped leaflets and disorganized Laminin-α5 matrix (Figures 6B and 6C; Table S1), similar to the valves observed in *Itga9* mutants. In wild-type controls at this developmental stage only a minor proportion of immature valves with rudimentary leaflets were observed, while in *Itga9*$^{-/-}$ mice approximately 90% of the valves were abnormal (Figure 6A; Table S1). While lymphatic valve defects were pronounced in the *Fn-EIIIA*$^{-/-}$ mice during early postnatal life, they diminished during progression into adulthood, coinciding with when the expression of FN-EIIIA is down-regulated. In the ear skin of three weeks old wild-type animal, punctuate staining, but no FN-EIIIA fibers, were detected in the lymphatic vessels and the valves (Figure 6D). At the same age the majority of the valves in *Fn-EIIIA* mutant animals had apparently normal leaflets when compared to the control (Figures 6E and 6F). The mice also exhibited otherwise normal lymphatic vasculature, including vessel diameter and smooth muscle cell coverage (Figures 6E and 6F). However, subcutaneous injection of FITC-dextran revealed reflux of dye from the collecting vessels, suggesting mild valve defects, and some morphologically abnormal valves in *Fn-EIIIA* deficient mice (Figures 6G-6I, 4/4 mice analyzed). These results suggest that *Fn-EIIIA* deficiency leads to lymphatic valve defects during embryonic and early postnatal life.

Integrin-α9-EIIIA interaction regulates FN assembly in lymphatic endothelial cells

The defective FN matrix observed in the *Itga9*$^{-/-}$ valves prompted us to examine the possibility that integrin-α9-EIIIA interaction contributes to FN assembly in lymphatic endothelial cells (LECs), despite the previous findings suggesting that the EIIIA domain is dispensable for matrix assembly in fibroblasts (Tan et al., 2004). We therefore tested whether primary human LECs are able to assemble their endogenously produced FN, which contains the EIIIA domain (Figure 7A). To avoid exogenous plasma FN lacking the EIIIA domain, the cells were grown in the presence of FN-depleted serum and fibril assembly was assessed by immunofluorescence for the EIIIA. After 24h in culture, a fibrillar FN-EIIIA network was detected on the surface of the LECs (Figure 7A). Inhibition of integrin-α9 function, or integrin-α9-EIIIA interaction, using blocking antibodies against integrin-α9 (Y9A2) or EIIIA (IST-9) (Figures 7A and 7B), or a blocking EIIIA peptide EDGIHEL (Liao et al., 2002)(data not shown), led to a significant decrease in FN-EIIIA fibril formation. *FN-EIIIA* levels were not reduced (Figures 7C), indicating that the defect was not due to impaired mRNA synthesis. A similar effect was seen when integrin-α9 expression was silenced using siRNA oligos (Figures 7A-7D). In contrast, inhibition of RGD-dependent integrin interactions, which have been considered essential for FN assembly via α5β1 and αv integrins, had no effect (Figure 7B), while siRNA-mediated knock-down of integrin-α5 (Figure 7D) partially blocked LEC mediated FN-EIIIA assembly (Figure 7A and 7B). Deoxycholate (DOC) differential solubilization assay and Western blot analysis were further used to analyse the conversion of DOC-soluble fibrils into insoluble stable matrix containing high molecular mass FN multimers. No DOC-insoluble material was associated with the LECs in which integrin-α9 expression or the integrin-α9-EIIIA interaction was blocked (Figure 7E, upper panel). Instead, similar quantities of DOC-soluble FN matrices were found in all cells (Figure 7E, lower panel). Consistent with the immunofluorescence data,

silencing of integrin-α5 expression partially blocked the formation of DOC-insoluble FN-EIIIA matrix (Figure 7E). These results suggest that although integrin-α5 cannot functionally compensate for the loss of integrin-α9, it contributes to FN fibrillogenesis in the LECs. However, the low levels of integrin-α5 detected in the developing lymphatic vessels (Figure 7F) suggest that it does not play a major role during valve morphogenesis. The above results demonstrate that integrin-α9-EIIIA interaction can directly regulate FN matrix assembly, suggesting a functionally indispensable, integrin-specific mechanism for FN fibrillogenesis in the LECs.

Discussion

The present study establishes integrin-α9 as an essential regulator of the morphogenetic process controlling the formation of lymphatic valve leaflets, which allow opening and closing of the valve in response to pressure changes. This action of the valve is critical for the maintenance of unidirectional lymphatic flow and the functionality of the entire lymphatic vascular system, highlighted by the lack or insufficient function of lymphatic valves as an underlying cause of human lymphedema (Alitalo et al., 2005).

The leaflets of a mature valve consist of a well-defined matrix in between two sheets of lymphatic endothelial cells, which forms a strong but elastic connective tissue core (Figure 1). During embryogenesis, the formation of the lymphatic valve is initiated by upregulation of FoxC2 and Prox1 transcription factors in distinct clusters of endothelial cells, which define the positions of future valves ((Norrmen et al., 2009), see Figure 5J). We found that the development of the valve leaflet is subsequently initiated by upregulation of integrin-α9 expression and deposition of ECM containing its ligand, the EIIIA splice isoform of FN. The localization of FN-EIIIA at the distal tip of the developing valve suggested its function in regulating valve leaflet elongation. However, from previous studies the precise function of FN-EIIIA has remained elusive. Despite strong expression in the angiogenic blood vessels, no vascular phenotypes were reported in *Fn-EIIIA* deficient mice (Astrof et al., 2004). *In vitro* studies demonstrated that inclusion of the EIIIA segment enhanced the ability of FN to incorporate into existing matrix (Guan et al., 1990). This suggests that FN-EIIIA may participate in FN fibrillogenesis, which is a highly regulated, multistep process initiated by binding of integrins to specific sites in the FN molecule (Leiss et al., 2008; Wierzbicka-Patynowski and Schwarzbauer, 2003). Studies in cultured cells have revealed that generation of cytoskeletal tension through integrin-mediated cell attachment and anchoring via focal adhesions causes a change in integrin-bound FN conformation that exposes cryptic self-association sites to allow FN fiber assembly (Leiss et al., 2008; Wierzbicka-Patynowski and Schwarzbauer, 2003). The small GTPases, including Rho and Rac, play critical roles in cytoskeletal tension generation via regulation of actin polymerization and myosin phosphorylation (Dzamba et al., 2009; Zhong et al., 1998). *In vivo*, tissue tension and FN fibrillogenesis can also be generated by cell-cell adhesion and cohesivity (Dzamba et al., 2009). The observation that FN assembly proceeded normally in *Fn-EIIIA* deficient fibroblasts (Tan et al., 2004) led to the conclusion that EIIIA domain is not required for matrix assembly (Leiss et al., 2008). Instead, fibril formation in these cells was most likely mediated through binding of the major FN receptor, integrin-α5β1, to the Arg-Gly-Asp

(RGD) motif located in the type III-10 module of FN (Fogerty et al., 1990), which has been considered the most important mechanism of FN assembly (Leiss et al., 2008).

Surprisingly, we found that in lymphatic endothelial cells the integrin-α9-EIIIA interaction directly regulated FN fibril assembly, while RGD-dependent interactions appeared dispensable for matrix formation. Although the EIIIA domain has not been previously implicated in FN fibrillogenesis, other RGD-independent mechanisms for FN assembly have been observed. In fact, the requirement of the RGD motif for the formation of a functional fibrillar FN network *in vivo* was recently challenged as it was found that mice expressing FN with a non-functional RGD motif assembled an apparently normal FN matrix (Takahashi et al., 2007). The assembly of the RGD-deficient FN was mediated via integrin-αvβ3 binding to NGR sequence in the fifth N-terminal type I module of FN, which is converted to a high affinity binding site through deamidation (Takahashi et al., 2007). In addition, binding of Mn^{2+} activated integrin-α4β1 to the CS-1 site of the alternatively spliced V region was shown to promote FN assembly *in vitro* (Sechler et al., 2000).

Our findings suggest that the defective FN matrix organization in *Itga9* mutant valves is a direct consequence of the lack of a specific integrin-matrix interaction and contributes to the observed defects in valve leaflet formation. In agreement, we found that a large proportion of lymphatic valves in neonatal *Fn-EIIIA* deficient mice displayed defective leaflets similar to those observed in the *Itga9* mutants. However, the absence of chylothorax and only partial recapitulation of the *Itga9*$^{-/-}$ phenotype suggest that the defect in lymphatic development in mice deficient of *Itga9* cannot be solely explained by a defect in EIIIA-containing FN matrix assembly. In particular, the observation that the valve defect in *Fn-EIIIA*$^{-/-}$ mice diminished in adulthood suggests that the animals can eventually overcome the requirement of FN-EIIIA, coinciding with when its expression is down-regulated. This may imply that during postnatal development other integrin-α9 ligand(s) become involved, or that FN fibrillogenesis can be mediated via alternative integrin-FN interactions. In agreement, we found that acute deletion of integrin-α9 postnatally in mature valves did not lead to degeneration of the leaflets within the one-week period investigated, suggesting that once the stable matrix fibrils are assembled, integrin-α9-EIIIA interaction is not required to maintain ECM organization and valve structure. However, our results do not exclude that integrin-α9-EIIIA is required for long-term maintenance of valves. Notably, although not normally present in adult tissues, FN-EIIIA is upregulated in various pathological situations, such as cancer, atherosclerosis and thrombosis (Muro et al., 2003; Tan et al., 2004; Villa et al., 2008). It is therefore likely that it is reactivated and plays a role also in adult lymphatic vessels under specific circumstances, for example during repair processes or when the vasculature is challenged by inflammation.

Why is integrin-α9 important specifically in valves? Unlike other parts of the lymphatic vasculature, which have thin or absent basement membranes, the discrete architecture of the connective tissue of a valve leaflet suggests specific requirement for highly regulated mechanism of matrix organization. Indeed, the development of a related structure, the heart valve, is known to rely on the formation of a highly organized ECM, and consequently, dysregulation of ECM, often caused by genetic defects in matrix protein structure or expression, is linked to heart valve disease (Armstrong and Bischoff, 2004; Lincoln et al.,

2006). FN assembly is likely to play a key role in coordinating the formation of complex matrices as it has been shown to initiate the organization of other ECM proteins, such as collagens, and control the stability of matrix fibers (Kadler et al., 2008; Sottile and Hocking, 2002). Our observations demonstrate that integrin-α9 is the predominant alpha subunit in lymphatic endothelia. Although the major FN receptor, integrin-α5, appeared to contribute to FN fibrillogenesis in the LECs *in vitro*, it was not able to functionally compensate for the loss of integrin-α9 either in cultured cells or *in vivo*. Low expression levels of integrin-α5 in the developing valves may provide one explanation for the dependency of these cells on alternative FN assembly pathways.

FN matrix assembly, as well as integrin-α9 signaling, promote adhesion-dependent cell growth and migration (Leiss et al., 2008; Liao et al., 2002; Singh et al., 2008; Sottile et al., 1998) and defects in these processes may therefore underlie the disrupted valve leaflet formation in *Itga9*$^{-/-}$ and *Fn-EIIIA*$^{-/-}$ mice. Although we cannot exclude a contribution of integrin-α9-mediated adhesion during the early events of valve formation, the observation that acute deletion of integrin-α9 in postnatal valves did not lead to cell detachment and degeneration of the valves argue against a role of integrin-α9 in mediating stable adhesion of valve endothelial cells *in vivo*. Furthermore, an *in vivo* BrdU incorporation assay showed that the valve endothelial cells expressing high levels of FoxC2, Prox1 and integrin-α9 do not proliferate during leaflet formation (E.B. and T.M., unpublished). These results suggest that endothelial cell adhesion and proliferation are unlikely to be controlled by integrin-α9 or involved in valve leaflet formation, respectively. Finally, the observed defect in valve leaflet elongation may be caused by failure in morphogenetic cell movements, which were shown to rely on proper organization of FN matrices in other developmental processes (Dzamba et al., 2009; Rozario et al., 2009). Therefore, we propose that the key function of the integrin-α9-EIIIA interaction is to provide an integrin-specific mechanism of FN matrix assembly and thereby coordinate ECM organization to allow formation of a leaflet of necessary length and strength, capable of supporting valve function.

In summary, we demonstrate that integrin-α9 and its ligand, FN-EIIIA, play specific roles in lymphatic valve development and remodeling into functional leaflets. To our knowledge, the only other mouse mutants identified to-date, which show a failure of valve formation, show additional lymphatic defects; mice lacking the C-terminal PDZ binding domain of ephrinB2 display vessel hyperplasia (Makinen et al., 2005) while *FoxC2* deficient mice have patterning defects (Norrmen et al., 2009; Petrova et al., 2004). The specific valve defects observed in the *Itga9* mutant mice therefore reveal a previously undescribed morphogenetic process and provide potential insights into the development of valves in other parts of the vascular system, such as in the veins and the heart, which are likely to be regulated by similar molecular mechanisms. Lack of integrin-α9 signaling in mice results ultimately in chylothorax and postnatal death (Huang et al., 2000). Recent identification of mutations in the *ITGA9* gene in fetuses with congenital chylothorax (Ma et al., 2008) suggests conservation of the signaling pathway from mice to human, making integrin-α9 a candidate gene for primary lymphedema caused by valve defects.

Experimental Procedures

Antibodies

The antibodies were rat antibodies to mouse PECAM-1 (MEC3.1, BD Biosciences), Tenascin-C (MTn-12, Abcam) and FoxC2 (Petrova et al., 2004); rabbit antibodies to mouse Fibronectin (Millipore), Laminin-α5 (Ringelmann et al., 1999) and LYVE-1 (Reliatch); rabbit antibodies to human Prox1 (Reliatech) and Fibronectin (Abcam); mouse antibodies to human cellular Fibronectin recognizing the EIIIA domain ((Liao et al., 2002), FN-3E2, Sigma and IST-9, Abcam), hamster antibody to mouse PECAM-1, goat antibodies to mouse integrin-α9 and Osteopontin (R&D Systems) and Cy3-conjugated mouse antibody against α-smooth muscle actin (Sigma). The monoclonal hamster antibody to mouse Podoplanin (8.1.1) developed by Andrew Farr was obtained from the Developmental Studies Hybridoma Bank. Secondary antibodies conjugated to Cy2, Cy3 or Cy5 were obtained from Jackson ImmunoResearch.

Mouse lines

Itga9$^{-/-}$ (Huang et al., 2000), *Itga9*^{lx} (Singh et al., 2008), *Vegfr3*$^{lz/+}$ (Dumont et al., 1998), *Fn-EIIIA*$^{-/-}$ (Muro et al., 2003), *Tnc*$^{-/-}$ (Forsberg et al., 1996), *Opn*$^{-/-}$ (Liaw et al., 1998), *Tie2-Cre* (Koni et al., 2001) and *Rosa26R* (Soriano, 1999) mice have been described previously. *VE-cadherin-CreER*^{T2} mice will be described elsewhere (R. Adams, unpublished). For the induction of Cre mediated recombination in newborn *VE-cadherin-CreER*^{T2} mice, 4-hydroxytamoxifen (4-OHT; 2 μl of 10 mg/ml dissolved in ethanol) was injected i.p. at P1 and P2 and the vessels were analyzed at P7-8. All animal experiments were performed in accordance with UK Home Office and institutional guidelines.

Immunostaining and X-Gal staining

For whole-mount staining, the tissue was fixed in 4% paraformaldehyde (PFA), permeabilized in 0.3% Triton-X100 in PBS (PBSTx) and blocked in 5% milk or serum. Primary antibodies were added to the blocking buffer and incubated with the tissue overnight at 4°C. After washes in PBSTx, the tissue was incubated with fluorochrome-conjugated secondary antibodies in the blocking buffer for 2h at RT, followed by washing in PBSTx and mounting in Mowiol. The samples were analyzed using Zeiss LSM 510 laser scanning confocal microscope. All confocal images, except Figures 5H, 5I and S4A-S4I, represent 2D projections of Z-stacks. Alternatively, biotin-conjugated secondary antibodies and ABC staining kit (Vector Laboratories) were used and the bound antibodies were visualized using diaminobenzidine (DAB) as a substrate. For histological analyses, skin biopsies were fixed in 4% PFA overnight, dehydrated and embedded in paraffin. Sections (5μm) were stained after heat-induced epitope retrieval using Tyramide Signal Amplification kit (TSA, NEN Life Sciences) and 3-Amino-9-Ethylcarbazole (AEC) as a substrate. For the visualization of lymphatic vessels in *Vegfr3*$^{lz/+}$ reporter mice, the tissues were fixed with 0.2% glutaraldehyde and stained by the β-galactosidase substrate X-gal (Promega).

Visualization of lymphatic vessel function

FITC-dextran (Sigma, 8 mg/mL in PBS) or FITC-conjugated *Lycopersicum Esculentum* lectin (Vector Laboratories, 1 mg/ml in PBS) was injected subcutaneously into an anesthetized mouse and the lymphatic vessels were analyzed by fluorescence microscopy.

Electron microscopy

The intestines were dissected from P5 mice and immediately fixed in 4% PFA/2.5% glutaraldehyde in 0.1M phosphate buffer pH 7.4. The samples were post fixed in reduced osmium tetroxide for 1 hour followed by 1% tannic acid in 0.05M sodium cacodylate for 45 minutes. Samples were then dehydrated through a graded series of ethanol and embedded in Araldite (Agar Scientific). Semi-thin sections were cut on a UCT ultramicrotome (Leica Microsystems UK), stained with 1% Toluidine Blue in 1% Borax and viewed under a III RS light microscope (Carl Zeiss UK) to locate the area of interest. Ultra-thin sections were cut and stained with lead citrate before being examined in a JEOL 1010 microscope and imaged with a Bioscan CCD (Gatan UK).

Cell culture

Human lymphatic endothelial cells (LEC) were isolated from primary dermal microvascular endothelial cell cultures (PromoCell) using rat antibody to human Podoplanin (NZ-1, Angiobio) and Mini/MidiMACS magnetic separation system (Miltenyi Biotech), as previously described (Makinen et al., 2001). The cells were cultured on fibronectin (Sigma) coated plates in the presence of 10 ng/ml VEGF-C (R&D Systems) and used at passages 4-6. For siRNA mediated knock-down, LECs were transfected twice during 48h using calcium phosphate (Dharmacon) in DMEM, supplemented with 20% FBS, followed by recovery in Endothelial Cell Medium (PromoCell) for 24h before the cells were used for experiments. ON-TARGETplus siRNAs were obtained from Dharmacon. The following targeting sequences were used: *ITGA9*_1: GAAGAAAGUCGUACUAUAG, *ITGA9*_2 GUGCAGAGAUGUUUCAUGU and *ITGA5*: UCACAUCGCUCUCAACUUC. Control transfections were carried out using ON-TARGETplus siControl Non-targeting siRNA from Dharmacon.

Analysis of FN fibril assembly

LECs in 5% FN-depleted serum were plated on glass coverslips. Similar results were obtained when the coverslips were coated with 0.2% gelatin (no exogenous FN) or with extracellular matrices extracted from *FN-EIIIA*$^{+/+}$ (Muro et al., 2003) embryonic fibroblasts (containing small quantities of exogenous FN, all of which contains the EIIIA domain). The function-blocking antibodies (mouse anti-human integrin-α9 (Y9A2; Millipore) and EIIIA (IST-9; Abcam)) and the blocking peptides were used at a concentration of 10 μg/ml. 24 hours after plating the cells were fixed in 4% PFA and FN fibril assembly was examined using immunofluorescence. Images from five randomly chosen view fields from two independent experiments were acquired. Image processing and analysis was performed using MetaMorph Imaging software (Molecular Devices). Scaled images were thresholded and filtered so that only FN-EIIIA-specific fibers greater than 4 pixels (1.8 μm) were recorded. The total fiber length per cell was calculated by dividing the total value recorded

with the number of cells present in each image. Isolation of DOC-soluble and – insoluble matrix was done as previously described (Wierzbicka-Patynowski et al., 2004). Equal amounts of total protein were separated by non-reducing 5% SDS-PAGE, transferred to nitrocellulose and probed with anti-EIIIA antibody (FN-3E2).

Western blot analysis

The cells were lysed in Triton-X100 lysis buffer (50 mM Tris pH 7.5, 120 mM NaCl, 10% glycerol, 1% TritonX-100) supplemented with Complete Protease Inhibitors (Roche). Lysates were clarified by centrifugation and subjected to immunoprecipitation and/or Western blot analysis using standard protocols. The antibodies were mouse antibody to human integrin-α5 (GBS5; Millipore) and human integrin-α9 (Y9A2; Millipore, for IP), chicken antibody to human integrin-α9 (GenWay, for WB) and mouse antibody to human α-tubulin (TAT-1). The bound antibodies were detected using HRP-conjugated secondary antibodies (Jackson ImmunoResearch) and ECL chemiluminescence.

Relative quantitative PCR

RNA from LECs was reverse transcribed using random hexamers and an avian myeloblastosis virus reverse transcriptase (Promega). cDNA was amplified by quantitative real-time PCR (ABI 7900HT) using SYBR Green PCR master mix reagent (Qiagen). Each primer was used at a concentration of 0.5 μM. Cycling conditions were as follows: step 1, 15 min at 95°C; step 2, 20 s at 94°C; step 3, 20 s at 60°C; step 4, 20 s at 72°C, with repeat from step 2 to step 4 35 times. Data from the reaction were collected and analyzed by the complementary computer software. Relative quantitations of gene expression were normalized to the endogenous control (*GAPDH*). The primers were *ITGA9*: 5′-CGGAATCATGTCTCCAACCT-3′ and 5′-TCTCTGCACCACCAGATGAG-3′, *EIIIA*: 5′-TTGATCGCCCTAAAGGACTG-3′ and 5′-ACCATCAGGTGCAGGGAATA-3′ and *GAPDH*: 5′-GAAGATGGTGATGGGATTTC-3′ and 5′-GAAGGTGAAGGTCGGAGT-3′.

Statistical analysis

P values were calculated using the non-parametric Mann-Whitney test, unpaired two-tailed Student T-test or χ^2 test as indicated.

Supplementary Material

Refer to Web version on PubMed Central for supplementary material.

Acknowledgments

We are grateful to K. Alitalo for the *Vegfr3*$^{lz/+}$ mice and R. Fässler, A. Faissner and T. Czopka for the *Tnc* mice and tissues. We thank I. Rosewell for help with the establishment of mouse colonies; H. Chapman, A. Horwood, E. Murray, S. Lighterness and C. Watkins for animal husbandry; and E. Nye for assistance with the histological analyses. We would like to thank M. Way, N. Hogg, M. Graupera and I. Ferby for helpful discussions and critical comments on the manuscript. This work has been supported by Cancer Research UK (E.B., S.X., A.W., R.A., T.M.) and by grant HL64353 from the National Heart Lung and Blood Institute (USA) (D.S.). The authors declare no financial conflict of interest.

References

Alitalo K, Tammela T, Petrova TV. Lymphangiogenesis in development and human disease. Nature. 2005; 438:946–953. [PubMed: 16355212]

Armstrong EJ, Bischoff J. Heart valve development: endothelial cell signaling and differentiation. Circ Res. 2004; 95:459–470. [PubMed: 15345668]

Astrof S, Crowley D, George EL, Fukuda T, Sekiguchi K, Hanahan D, Hynes RO. Direct test of potential roles of EIIIA and EIIIB alternatively spliced segments of fibronectin in physiological and tumor angiogenesis. Mol Cell Biol. 2004; 24:8662–8670. [PubMed: 15367684]

Avraamides CJ, Garmy-Susini B, Varner JA. Integrins in angiogenesis and lymphangiogenesis. Nat Rev Cancer. 2008; 8:604–617. [PubMed: 18497750]

Dumont DJ, Jussila L, Taipale J, Lymboussaki A, Mustonen T, Pajusola K, Breitman M, Alitalo K. Cardiovascular failure in mouse embryos deficient in VEGF receptor-3. Science. 1998; 282:946–949. [PubMed: 9794766]

Dzamba BJ, Jakab KR, Marsden M, Schwartz MA, DeSimone DW. Cadherin adhesion, tissue tension, and noncanonical Wnt signaling regulate fibronectin matrix organization. Dev Cell. 2009; 16:421–432. [PubMed: 19289087]

Ferrell RE, Levinson KL, Esman JH, Kimak MA, Lawrence EC, Barmada MM, Finegold DN. Hereditary lymphedema: evidence for linkage and genetic heterogeneity. Hum Mol Genet. 1998; 7:2073–2078. [PubMed: 9817924]

Finegold DN, Kimak MA, Lawrence EC, Levinson KL, Cherniske EM, Pober BR, Dunlap JW, Ferrell RE. Truncating mutations in FOXC2 cause multiple lymphedema syndromes. Hum Mol Genet. 2001; 10:1185–1189. [PubMed: 11371511]

Fogerty FJ, Akiyama SK, Yamada KM, Mosher DF. Inhibition of binding of fibronectin to matrix assembly sites by anti-integrin (alpha 5 beta 1) antibodies. J Cell Biol. 1990; 111:699–708. [PubMed: 2380248]

Forsberg E, Hirsch E, Frohlich L, Meyer M, Ekblom P, Aszodi A, Werner S, Fassler R. Skin wounds and severed nerves heal normally in mice lacking tenascin-C. Proc Natl Acad Sci U S A. 1996; 93:6594–6599. [PubMed: 8692862]

Francois M, Caprini A, Hosking B, Orsenigo F, Wilhelm D, Browne C, Paavonen K, Karnezis T, Shayan R, Downes M, et al. Sox18 induces development of the lymphatic vasculature in mice. Nature. 2008; 456:643–647. [PubMed: 18931657]

Geiger B, Bershadsky A, Pankov R, Yamada KM. Transmembrane crosstalk between the extracellular matrix--cytoskeleton crosstalk. Nat Rev Mol Cell Biol. 2001; 2:793–805. [PubMed: 11715046]

Guan JL, Trevithick JE, Hynes RO. Retroviral expression of alternatively spliced forms of rat fibronectin. J Cell Biol. 1990; 110:833–847. [PubMed: 2307710]

Huang XZ, Wu JF, Ferrando R, Lee JH, Wang YL, Farese RV Jr, Sheppard D. Fatal bilateral chylothorax in mice lacking the integrin alpha9beta1. Mol Cell Biol. 2000; 20:5208–5215. [PubMed: 10866676]

Hynes RO. Cell-matrix adhesion in vascular development. J Thromb Haemost. 2007; 5(1):32–40. [PubMed: 17635706]

Irrthum A, Devriendt K, Chitayat D, Matthijs G, Glade C, Steijlen PM, Fryns JP, Van Steensel MA, Vikkula M. Mutations in the transcription factor gene SOX18 underlie recessive and dominant forms of hypotrichosis-lymphedema-telangiectasia. Am J Hum Genet. 2003; 72:1470–1478. [PubMed: 12740761]

Jurisic G, Detmar M. Lymphatic endothelium in health and disease. Cell Tissue Res. 2009; 335:97–108. [PubMed: 18648856]

Kadler KE, Hill A, Canty-Laird EG. Collagen fibrillogenesis: fibronectin, integrins, and minor collagens as organizers and nucleators. Curr Opin Cell Biol. 2008; 20:495–501. [PubMed: 18640274]

Karkkainen MJ, Saaristo A, Jussila L, Karila KA, Lawrence EC, Pajusola K, Bueler H, Eichmann A, Kauppinen R, Kettunen MI, et al. A model for gene therapy of human hereditary lymphedema. Proc Natl Acad Sci U S A. 2001; 98:12677–12682. [PubMed: 11592985]

Koni PA, Joshi SK, Temann UA, Olson D, Burkly L, Flavell RA. Conditional vascular cell adhesion molecule 1 deletion in mice: impaired lymphocyte migration to bone marrow. J Exp Med. 2001; 193:741–754. [PubMed: 11257140]

Lauweryns JM, Boussauw L. The ultrastructure of lymphatic valves in the adult rabbit lung. Z Zellforsch Mikrosk Anat. 1973; 143:149–168. [PubMed: 4761509]

Leiss M, Beckmann K, Giros A, Costell M, Fassler R. The role of integrin binding sites in fibronectin matrix assembly in vivo. Curr Opin Cell Biol. 2008; 20:502–507. [PubMed: 18586094]

Liao YF, Gotwals PJ, Koteliansky VE, Sheppard D, Van De Water L. The EIIIA segment of fibronectin is a ligand for integrins alpha 9beta 1 and alpha 4beta 1 providing a novel mechanism for regulating cell adhesion by alternative splicing. J Biol Chem. 2002; 277:14467–14474. [PubMed: 11839764]

Liaw L, Birk DE, Ballas CB, Whitsitt JS, Davidson JM, Hogan BL. Altered wound healing in mice lacking a functional osteopontin gene (spp1). J Clin Invest. 1998; 101:1468–1478. [PubMed: 9525990]

Lincoln J, Lange AW, Yutzey KE. Hearts and bones: shared regulatory mechanisms in heart valve, cartilage, tendon, and bone development. Dev Biol. 2006; 294:292–302. [PubMed: 16643886]

Ma GC, Liu CS, Chang SP, Yeh KT, Ke YY, Chen TH, Wang BB, Kuo SJ, Shih JC, Chen M. A recurrent ITGA9 missense mutation in human fetuses with severe chylothorax: possible correlation with poor response to fetal therapy. Prenat Diagn. 2008; 28:1057–1063. [PubMed: 18973153]

Makinen T, Adams RH, Bailey J, Lu Q, Ziemiecki A, Alitalo K, Klein R, Wilkinson GA. PDZ interaction site in ephrinB2 is required for the remodeling of lymphatic vasculature. Genes Dev. 2005; 19:397–410. [PubMed: 15687262]

Makinen T, Veikkola T, Mustjoki S, Karpanen T, Catimel B, Nice EC, Wise L, Mercer A, Kowalski H, Kerjaschki D, et al. Isolated lymphatic endothelial cells transduce growth, survival and migratory signals via the VEGF-C/D receptor VEGFR-3. Embo J. 2001; 20:4762–4773. [PubMed: 11532940]

Muro AF, Chauhan AK, Gajovic S, Iaconcig A, Porro F, Stanta G, Baralle FE. Regulated splicing of the fibronectin EDA exon is essential for proper skin wound healing and normal lifespan. J Cell Biol. 2003; 162:149–160. [PubMed: 12847088]

Navas V, O'Morchoe PJ, O'Morchoe CC. Lymphatic valves of the rat pancreas. Lymphology. 1991; 24:146–154. [PubMed: 1791725]

Norrmen C, Ivanov KI, Cheng J, Zangger N, Delorenzi M, Jaquet M, Miura N, Puolakkainen P, Horsley V, Hu J, et al. FOXC2 controls formation and maturation of lymphatic collecting vessels through cooperation with NFATc1. J Cell Biol. 2009; 185:439–457. [PubMed: 19398761]

Pagani F, Zagato L, Vergani C, Casari G, Sidoli A, Baralle FE. Tissue-specific splicing pattern of fibronectin messenger RNA precursor during development and aging in rat. J Cell Biol. 1991; 113:1223–1229. [PubMed: 2040649]

Petrova TV, Karpanen T, Norrmen C, Mellor R, Tamakoshi T, Finegold D, Ferrell R, Kerjaschki D, Mortimer P, Yla-Herttuala S, et al. Defective valves and abnormal mural cell recruitment underlie lymphatic vascular failure in lymphedema distichiasis. Nat Med. 2004; 10:974–981. [PubMed: 15322537]

Ringelmann B, Roder C, Hallmann R, Maley M, Davies M, Grounds M, Sorokin L. Expression of laminin alpha1, alpha2, alpha4, and alpha5 chains, fibronectin, and tenascin-C in skeletal muscle of dystrophic 129ReJ dy/dy mice. Exp Cell Res. 1999; 246:165–182. [PubMed: 9882526]

Rozario T, Dzamba B, Weber GF, Davidson LA, DeSimone DW. The physical state of fibronectin matrix differentially regulates morphogenetic movements in vivo. Dev Biol. 2009; 327:386–398. [PubMed: 19138684]

Sechler JL, Cumiskey AM, Gazzola DM, Schwarzbauer JE. A novel RGD-independent fibronectin assembly pathway initiated by alpha4beta1 integrin binding to the alternatively spliced V region. J Cell Sci. 2000; 113(Pt 8):1491–1498. [PubMed: 10725231]

Singh P, Chen C, Pal-Ghosh S, Stepp MA, Sheppard D, Van De Water L. Loss of Integrin alpha9beta1 Results in Defects in Proliferation, Causing Poor Re-Epithelialization during Cutaneous Wound Healing. J Invest Dermatol. 2008

Soriano P. Generalized lacZ expression with the ROSA26 Cre reporter strain. Nat Genet. 1999; 21:70–71. [PubMed: 9916792]

Sottile J, Hocking DC. Fibronectin polymerization regulates the composition and stability of extracellular matrix fibrils and cell-matrix adhesions. Mol Biol Cell. 2002; 13:3546–3559. [PubMed: 12388756]

Sottile J, Hocking DC, Swiatek PJ. Fibronectin matrix assembly enhances adhesion-dependent cell growth. J Cell Sci. 1998; 111(Pt 19):2933–2943. [PubMed: 9730985]

Takahashi S, Leiss M, Moser M, Ohashi T, Kitao T, Heckmann D, Pfeifer A, Kessler H, Takagi J, Erickson HP, et al. The RGD motif in fibronectin is essential for development but dispensable for fibril assembly. J Cell Biol. 2007; 178:167–178. [PubMed: 17591922]

Tammela T, Saaristo A, Holopainen T, Lyytikka J, Kotronen A, Pitkonen M, Abo-Ramadan U, Yla-Herttuala S, Petrova TV, Alitalo K. Therapeutic differentiation and maturation of lymphatic vessels after lymph node dissection and transplantation. Nat Med. 2007; 13:1458–1466. [PubMed: 18059280]

Tan MH, Sun Z, Opitz SL, Schmidt TE, Peters JH, George EL. Deletion of the alternatively spliced fibronectin EIIIA domain in mice reduces atherosclerosis. Blood. 2004; 104:11–18. [PubMed: 14976060]

Villa A, Trachsel E, Kaspar M, Schliemann C, Sommavilla R, Rybak JN, Rosli C, Borsi L, Neri D. A high-affinity human monoclonal antibody specific to the alternatively spliced EDA domain of fibronectin efficiently targets tumor neo-vasculature in vivo. Int J Cancer. 2008; 122:2405–2413. [PubMed: 18271006]

Wierzbicka-Patynowski I, Mao Y, Schwarzbauer JE. Analysis of fibronectin matrix assembly. Curr Protoc Cell Biol. 2004; Chapter 10 Unit 10 12.

Wierzbicka-Patynowski I, Schwarzbauer JE. The ins and outs of fibronectin matrix assembly. J Cell Sci. 2003; 116:3269–3276. [PubMed: 12857786]

Yokosaki Y, Matsuura N, Higashiyama S, Murakami I, Obara M, Yamakido M, Shigeto N, Chen J, Sheppard D. Identification of the ligand binding site for the integrin alpha9 beta1 in the third fibronectin type III repeat of tenascin-C. J Biol Chem. 1998; 273:11423–11428. [PubMed: 9565552]

Yokosaki Y, Matsuura N, Sasaki T, Murakami I, Schneider H, Higashiyama S, Saitoh Y, Yamakido M, Taooka Y, Sheppard D. The integrin alpha(9)beta(1) binds to a novel recognition sequence (SVVYGLR) in the thrombin-cleaved amino-terminal fragment of osteopontin. J Biol Chem. 1999; 274:36328–36334. [PubMed: 10593924]

Zhong C, Chrzanowska-Wodnicka M, Brown J, Shaub A, Belkin AM, Burridge K. Rho-mediated contractility exposes a cryptic site in fibronectin and induces fibronectin matrix assembly. J Cell Biol. 1998; 141:539–551. [PubMed: 9548730]

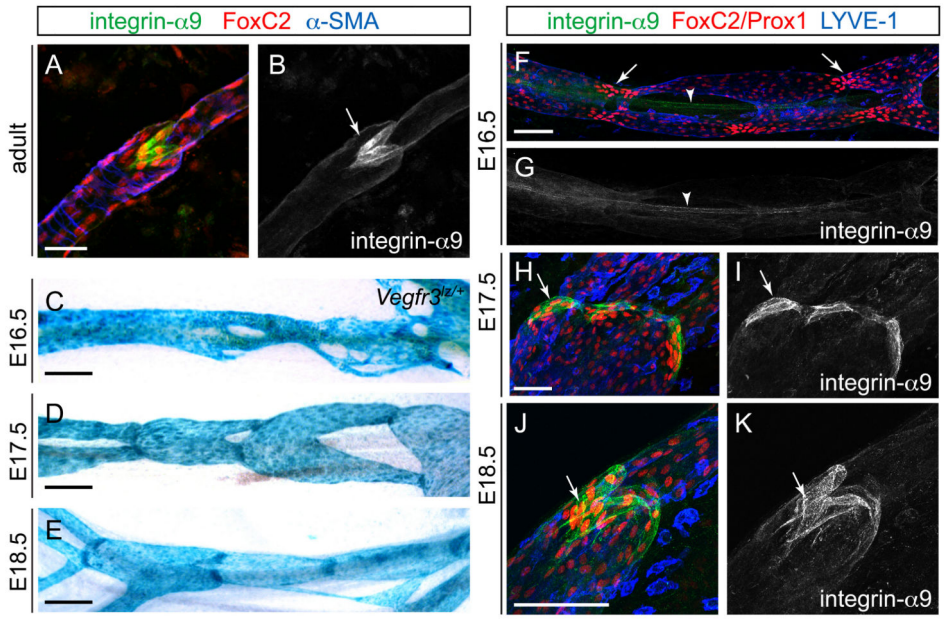

Figure 1. Expression of integrin-α9 in mature and developing lymphatic valves

(A, B) Immunofluorescence staining of adult ear skin with antibodies against integrin-α9 (green), FoxC2 (red) and α-smooth muscle actin (α-SMA, blue). Arrow in (B) points to a luminal valve. (C-E) Development of mesenteric lymphatic vessels. Whole-mount X-Gal staining of mesenteric lymphatic vessels from *Vegfr3*$^{lz/+}$ embryos. The tissues were taken from embryos at the indicated ages (E16.5-E18.5).

(F-K) Immunofluorescence staining of developing mesenteric lymphatic vessels of E16.5 (F, G), E17.5 (H, I) and E18.5 (J, K) with antibodies against integrin-α9 (green), Prox1 (F, red) or FoxC2 (H, J, red) and LYVE-1 (F, H, J, blue). Arrowhead in (F, G) points to a blood vessel, the smooth muscle coverage of which is positive for integrin-α9 staining. Arrows point to clusters of cells expressing high levels of Prox1 and FoxC2.

Scale bars; A, B, H-K: 50 μm, C-G: 1 mm.

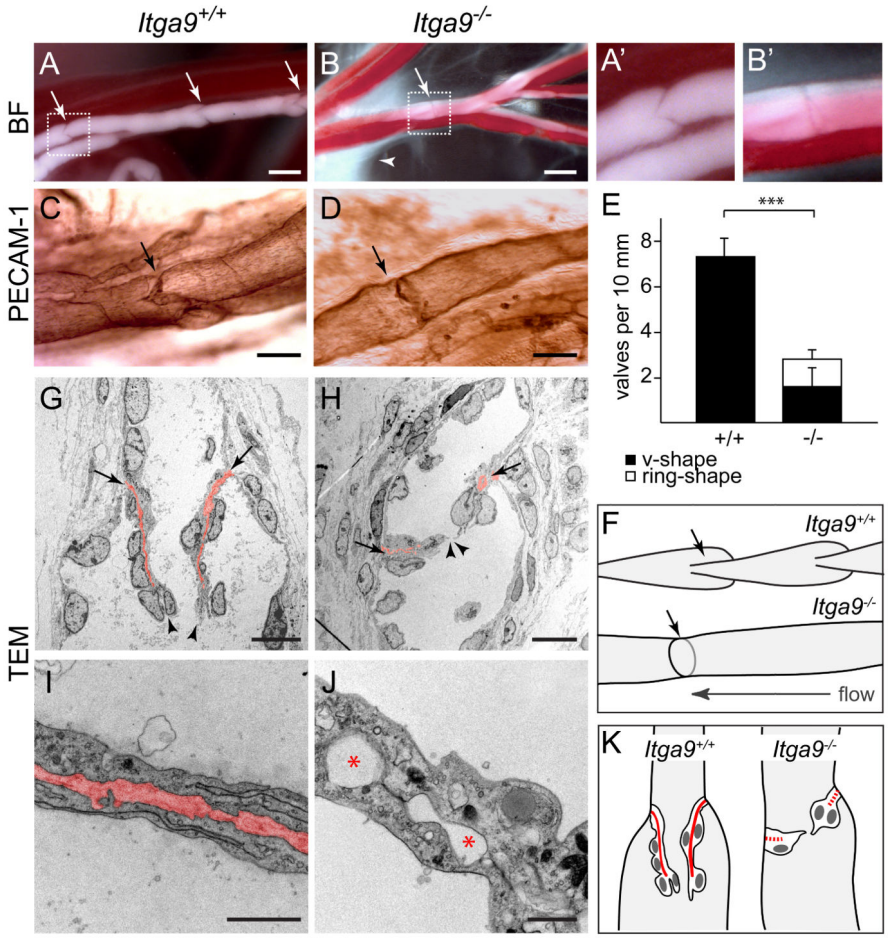

Figure 2. Abnormal valves in *Itga9* deficient mice

(A-B′) Luminal valves in chyle-filled mesenteric lymphatic vessels of wild-type (A, A′) and *Itga9* mutant mice (B, B′). Note the difference in the shape of a wild-type in comparison to a mutant valve (A′, B′, arrows in A, B) and leakage of chyle from the mutant vessels (arrowhead in B). BF = bright field.

(C, D) PECAM-1 immunohistochemistry of P5 mesenteric vessels and luminal valves (arrow) in wild-type (C) and *Itga9*$^{-/-}$ (D) mice.

(E) Quantification of the number of luminal valves in P5 wild-type and *Itga9*$^{-/-}$ mesenteric lymphatic vessels (mean ± s.d., n = 4 animals per genotype, 3 vessels each). Black bar = normal V-shaped valves; white bar = abnormal valves with ring appearance. *** $p < 0.0001$ (Mann-Whitney test).

(F) Schematic representation of luminal valves (arrows) in the collecting lymphatic vessels of *Itga9*$^{+/+}$ and *Itga9*$^{-/-}$ mice.

(G-J) Transmission electron micrographs of wild-type (G, I) and *Itga9*$^{-/-}$ (H, J) valves in mesenteric lymphatic vessels of P6 mice. Arrows in (G, H) point to the matrix core (red) anchored into the vessels wall, arrowheads mark the free edges of the valve leaflets. (I) shows the valve leaflet with a connective tissue core (red). Note the rudimentary (arrows in H) or absent (J) matrix core in the mutant valves and the gaps in between the two endothelial sheets (red asterisks in J).

(K) Schematic representation of luminal valves in the *Itga9*$^{+/+}$ and *Itga9*$^{-/-}$ mice. Matrix core is indicated in red.

Scale bars; A, B: 100 μm, C, D: 50 μm, G, H: 10 μm, I, J: 1 μm.

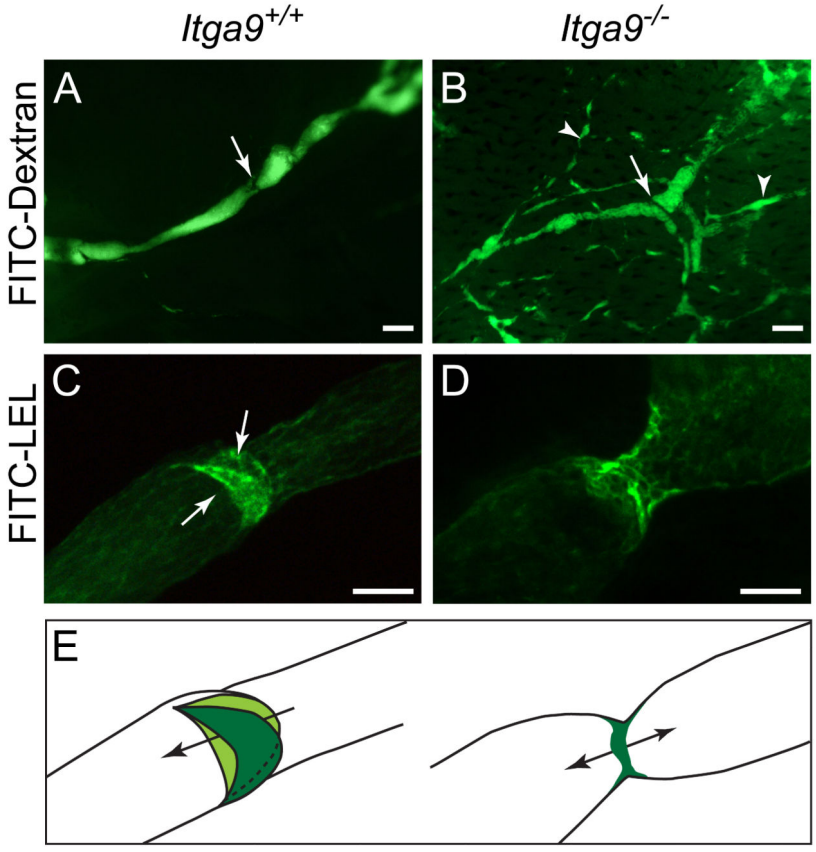

Figure 3. Defective lymphatic drainage in *Itga9* deficient mice

(A, B) Visualisation of dermal collecting vessels following injection of FITC-dextran into the footpads of P6 wild-type (A) and *Itga9*$^{-/-}$ mice (B). Note the presence of an abnormal vessel network (arrowheads in B) and a valve in a vessel branch point in the *Itga9* mutants (arrow in B).

(C, D) FITC-lectin (LEL) staining of the valves in dermal lymphatic vessels following footpad injection. No valve leaflets are seen in the *Itga9* mutant (D). Arrows in (C) point to the two valve leaflets seen from the 90° angle when compared to Figure 2A, D.

(E) Schematic representation of a side view of luminal valves as visualized by FITC-LEL staining in the collecting lymphatic vessels of *Itga9*$^{+/+}$ (left) and *Itga9*$^{-/-}$ (right) mice. Arrows indicate the direction of the flow.

Scale bars; A, B: 100 μm, C, D: 50 μm.

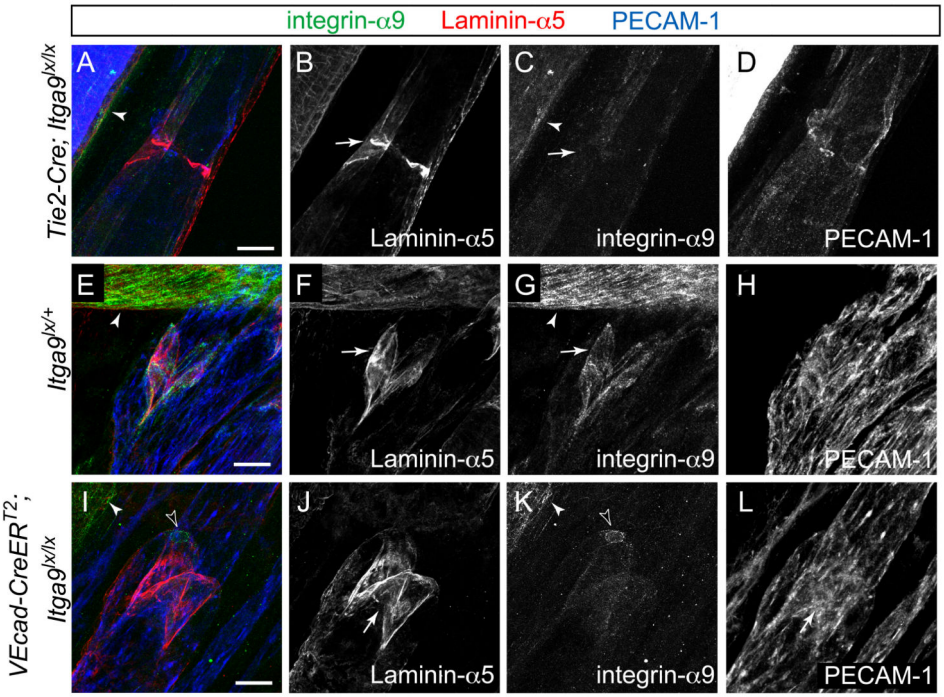

Figure 4. Endothelial cell specific deletion of *Itga9* during development and in mature valves

Lymphatic vessels of *Tie2-Cre;Itga9$^{lx/lx}$* mouse (A-D), and of 4-OHT treated *Itga9$^{lx/+}$* (E-H) and *VEcad-CreER^{T2}; Itga9$^{lx/lx}$* (I-L) mice stained with antibodies against Laminin-α5 (red), integrin-α9 (green) and PECAM-1 (blue). Expression of integrin-α9 is detected in the vascular SMC (arrowhead in A, C, E, G, I, K) but is lost from the endothelial cells in *Tie2-Cre;Itga9$^{lx/lx}$* (C) and from most endothelial cells of the valves of *VEcad-CreER^{T2}; Itga9$^{lx/lx}$* mutant animals (I, K, open arrowhead points to a single integrin-α9 expressing cell). Note the abnormal valve in *Tie2-Cre;Itga9$^{lx/lx}$* mouse (arrow in B), which has undergone embryonic deletion of *Itga9* allele, but intact valve leaflets (arrow in J) and the attachment of LECs on the leaflets in the *VEcad-CreER^{T2}; Itga9$^{lx/lx}$* mutant (arrow in L), which has undergone postnatal deletion of *Itga9* allele, as compared to a control (arrows in F, G). Scale bars; A-L: 20 μm.

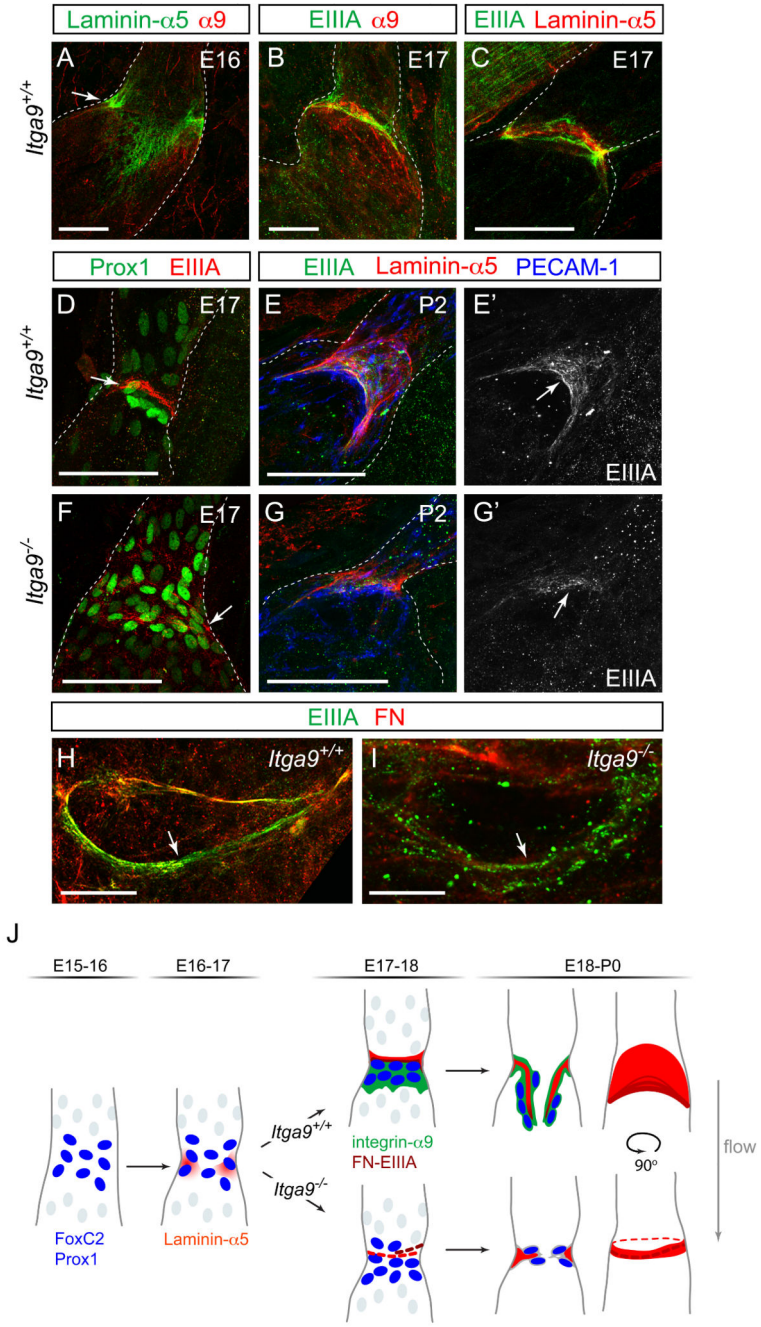

Figure 5. Development of lymphatic valve leaflets in wild-type and *Itga9*$^{-/-}$ mice

(A-C) Immunofluorescence staining of developing mesenteric lymphatic vessels of E16 (A) and E17 (B, C) wild-type embryo using antibodies against Laminin-α5, integrin-α9 and FN-EIIIA (colors as indicated). The dotted lines outline the vessels.

(D-G) Immunolabeling of lymphatic valves in wild-type (D-E′) and *Itga9*$^{-/-}$ (F-G′) mesenteric vessels for Prox1 (green) and FN-EIIIA (red; E, F; at E17) or for Laminin-α5 (red), FN-EIIIA (green) and the endothelial marker PECAM-1 (blue; E, G; at P2). The arrows in (D, E′, F, G′) point to FN-EIIIA fibers.

(H, I) View through the opening of the valve in P0 wild-type (H) and *Itga9*$^{-/-}$ (I) vessels, labelled for FN (red) and FN-EIIIA (green). Note the punctuate localization of FN-EIIIA in the *Itga9*$^{-/-}$ valve (arrow in I) compared to the fibrous staining in the wild-type (arrow in H). (J) Schematic model of lymphatic valve formation. Upregulation of Prox1 and FoxC2 transcription factors (blue nuclei) in lymphatic vessels define the positions of future valves. Deposition of extracellular matrix (red) containing Laminin-α5 and FN-EIIIA and re-orientation of cells expressing high levels of Prox1 and FoxC2 perpendicular to the vessel wall is followed by upregulation of integrin-α9 (green) on the outflow side of the future valve. *Itga9*$^{-/-}$ mice (below) display defective organization of the extracellular matrix and failure of leaflet formation.

Scale bars; A-G: 50 μm, H, I: 10 μm.

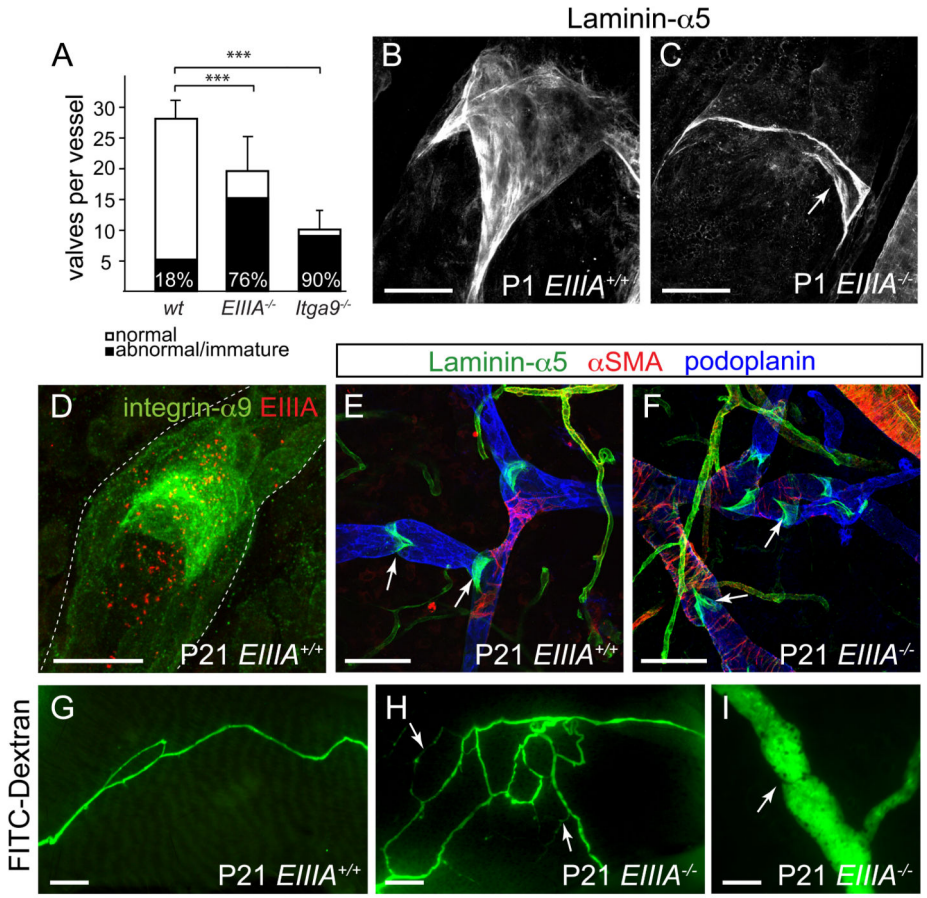

Figure 6. Abnormal lymphatic valves in mice lacking the integrin-α9 ligand, FN-EIIIA

(A) Luminal valve numbers in newborn wild-type, *Fn-EIIIA*$^{-/-}$ and *Itga9*$^{-/-}$ mesenteric lymphatic vessels (mean ± s.d., n ≥ 4 animals per genotype, ≥ 2 vessels each, see Suppl. Table 1). The percentage of abnormal valves is indicated: *** $p < 0.0001$ (χ^2 test).

(B, C) Visualization of lymphatic valves in P1 wild-type (B) and *Fn-EIIIA*$^{-/-}$ (C) mesenteric vessels using antibodies against Laminin-α5. Note the incomplete development of the valve as evident by lack of leaflets (arrow in C) in the *Fn-EIIIA*$^{-/-}$ vessels.

(D) Immunofluorescence staining of three weeks old ear skin for integrin-α9 (green) and EIIIA (red).

(E, F) Dermal lymphatic vessels in the ears of three weeks old wild-type (E) and *Fn-EIIIA*$^{-/-}$ (F) mice labeled for Laminin-α5 (green), podoplanin (blue) and α-SMA (red).

(G-I) FITC-dextran assay in three weeks old wild-type (G) and *Fn-EIIIA*$^{-/-}$ mice (H, I). Note the reflux of dye (arrows in H) and an abnormal valve (arrow in I) in the mutant skin.

Scale bars; B, C: 20 μm, D:50μm, E, F, I: 100 μm, G, H: 400 μm.

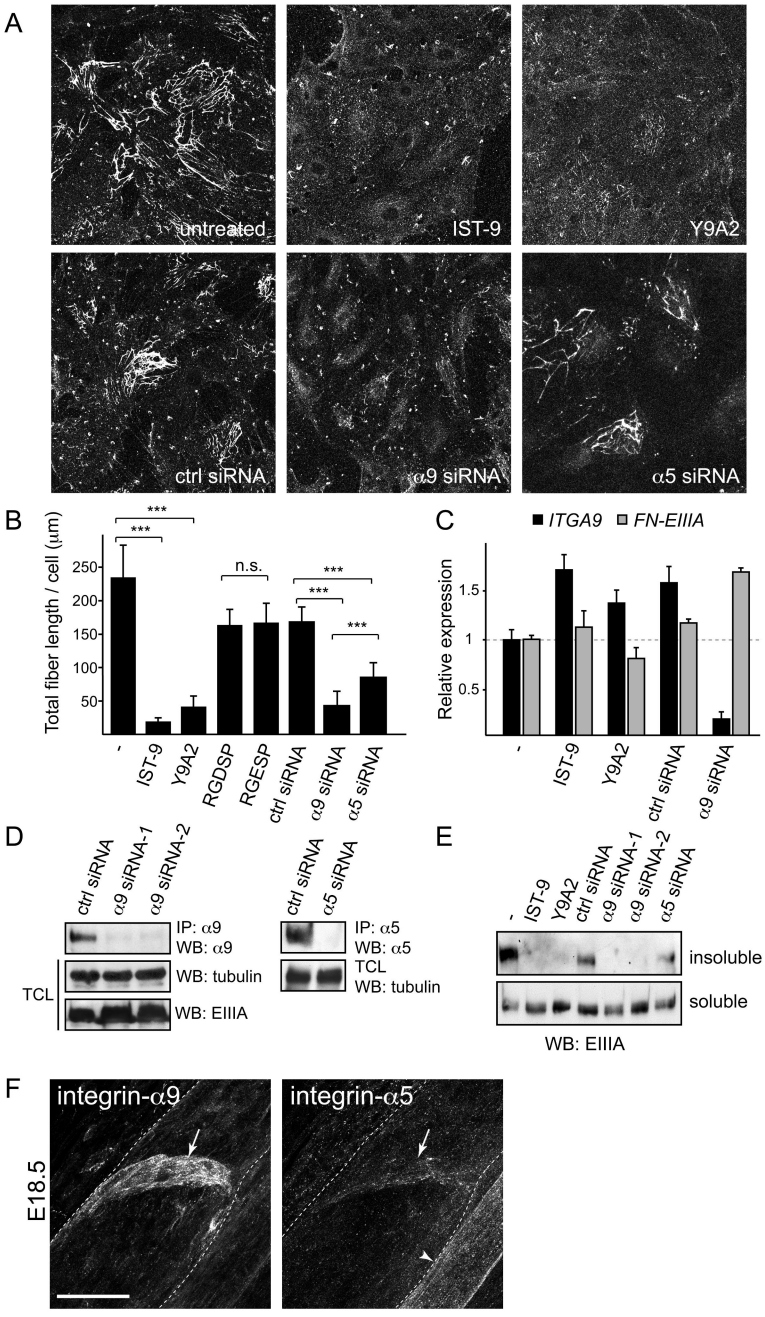

Figure 7. Integrin-α9-EIIIA interaction regulates FN fibril assembly in primary human lymphatic endothelial cells

(A) FN fibrils in primary human lymphatic endothelial cells (LECs). Integrin-α9-EIIIA interaction was blocked using antibodies against EIIIA (IST-9) or integrin-α9β1 (Y9A2), or siRNA against integrin-α9 or -α5, and stained with EIIIA antibodies.

(B) Quantification of FN fibrillogenesis in the LECs, in which integrin-α9-EIIIA interaction (IST-9, Y9A2, α9 siRNA) or integrin-α5/RGD-dependent integrin interactions (RGDSP peptide, α5 siRNA) were inhibited, in comparison to the control cells (untreated, ctrl siRNA or RGESP peptide). Data represent mean FN-EIIIA fiber length per cell (± s.d) from five

randomly chosen view fields in two independent experiments. *** $p < 0.003$, n.s.= non-significant, $p = 0.881$ (Student T-test).

(C) qPCR of *ITGA9* and *FN-EIIIA* in human LECs. Data represent mean ± s.d. of triplicates.

(D) siRNA mediated knock-down of integrin expression in primary human LECs. Western blot analysis of immunoprecipitated (IP) cell lysates using integrin-α9 or -α5 antibodies (upper panels). For the loading control, the total cell lysates (TCL) were blotted against α-tubulin and EIIIA.

(E) Conversion of DOC-soluble FN fibrils into insoluble stable matrix. DOC-insoluble (upper panel) and -soluble matrix (lower panel) isolated from the LECs were separated in non-reducing SDS-PAGE and probed for EIIIA.

(F) Immunofluorescent staining of wild type E18 mesenteric vessels using antibodies against integrin-α9 (left panel) and integrin-α5 (right panel). Note low levels of integrin-α5 expression in the valve (arrows) in comparison to strong staining in the blood vessel endothelia (arrowhead).

Scale bar = 20 μm.